Dalton Transactions

RSC Publishing

PAPER

View Article Online
View Journal | View Issue

Cite this: *Dalton Trans.*, 2013, **42**, 15670

Synthesis, structure, and reactivity of tris(amidate) mono(amido) and tetrakis(amidate) complexes of group 4 transition metals†

Philippa R. Payne, Robert K. Thomson, Diane M. Medeiros, Geoff Wan and Laurel L. Schafer*

Received 10th July 2013,
Accepted 9th September 2013

DOI: 10.1039/c3dt51868j

www.rsc.org/dalton

The syntheses of a series of tris(amidate) mono(amido) titanium and zirconium complexes are reported. The binding motif of the amidate ligand has been determined to depend on the size of the metal centre for these sterically demanding *N*,*O*-chelating ligands; the larger zirconium metal centre supports three κ^2-(*N*,*O*) bound amidate ligands while the titanium analogue has one ligand bound in a κ^1-(*O*) fashion to alleviate steric strain. Reactivity studies indicate that, despite high steric crowding about the tris(amidate) mono(amido) zirconium metal centre, transamination of the reactive dimethylamido ligand can be achieved using aniline. This complex is also an active precatalyst for intramolecular alkene hydroamination, in which protonolysis of one amidate ligand in the presence of excess amine is observed as an initiation step prior to catalytic turnover. Eight-coordinate homoleptic κ^2-amidate complexes of zirconium and hafnium have also been prepared.

Introduction

In recent years, we and others have reported the synthesis of a variety of monometallic mono and bis(*N*,*O*)-ligated group 3, 4, and 5 metal complexes with broad applications in catalysis.[1–10] These complexes include mono and bis(amidate) tantalum(v) complexes for the hydroaminoalkylation of amines,[10,11] mono and bis(amidate) yttrium(iii) complexes for the hydroamination of aminoalkenes[9,12] and the amidation of aldehydes,[13] bis-(2-pyridonate) titanium(iv) complexes for the random copolymerization of ε-caprolactone and *rac*-lactide,[14] bis(ureate) zirconium(iv) complexes[15,16] as well as bis(amidate) zirconium(iv) and titanium(iv) complexes for hydroamination[7,12,15–22] and olefin polymerization.[2] These complexes can be generated from the homoleptic metal amide or alkyl starting materials ($M(NR_2)_x$ or MR_x) *via* a protonolysis reaction (Scheme 1) with the organic proligand. In most cases, merely adjusting the ligand to metal stoichiometry allows for the selective generation of targeted metal complexes.

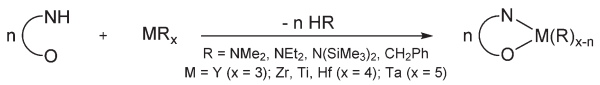

Scheme 1 Protonolysis methodology using homoleptic metal amido or alkyl starting materials.

Tris(amidate) yttrium complexes have been used to catalyze the polymerization of ε-caprolactone[23] and *rac*-lactide[14] as well as the amidation of aldehydes.[13] However, to date, tris(*N*,*O*)-ligated group 4 systems have not been investigated. In an effort to further explore the coordination chemistry of group 4 amidate complexes, here we investigate the synthesis, characterization, and reactivity of sterically crowded tris(amidate) mono(amido) complexes. In some cases, even tetrakis(amidate) complexes can be readily prepared.

Amidate ligands can adopt a variety of coordination modes when binding to a metal; the ligands can bind in a monodentate fashion, either κ^1-(*O*) or κ^1-(*N*), or in a bidentate κ^2-(*N*,*O*) motif, generating a four-membered metallacycle. When the chelating binding mode is achieved, despite the large steric requirements of the ligand and the small size of the group 4 d^0 metal centres, complexes with expanded coordination numbers often result. The structure and coordination geometry of these complexes in both the solution phase and the solid state are of particular interest. Here we report trends in amidate group 4 metal coordination and we show how both metal and ligand size can impact observed bonding modes. The resultant reactivity of these sterically congested complexes

Department of Chemistry, University of British Columbia, 2036 Main Mall, Vancouver, BC, Canada, V6 T 1Z1. E-mail: schafer@chem.ubc.ca; Fax: +1 (604)-822-2847; Tel: +1 (604)-822-9264

†Electronic supplementary information (ESI) available: Details of the crystal structure determination of **1**, **4**, **5**, **6**, and **7**, variable temperature NMR spectra for **1**, and representative spectra for the intramolecular hydroamination. CCDC 958398, 943792, 943794–943796. For ESI and crystallographic data in CIF or other electronic format see DOI: 10.1039/c3dt51868j

is reported and most importantly, the reactivity of these systems in catalytic hydroamination is explored.

Results and discussion

Coordination chemistry

Previous work has described the synthesis of bis(*N*-(2,6-diisopropylphenyl)benzamidate) bis(diethylamido) titanium, a robust catalyst for the hydroamination of alkynes,[17,18,24,25] *via* a protonolysis reaction of titanium tetrakis(diethylamido) with the amide proligand. The amidate ligands in this monometallic complex are bound in a κ^2 fashion in the solid state and the steric bulk of the nitrogen substituent helps to avoid bridging interactions. Application of this strategy for the synthesis of mono(amidate) tris(amido) complexes of group 4 metals has not been successful, and instead complex product mixtures result. However, such protonolysis reactions may be used for the synthesis of tris(amidate) complexes. *N*-(2,6-Dimethylphenyl)benzamide is an ideal proligand for this application as the slightly reduced steric bulk of the nitrogen-bound aryl substituent is attractive for potentially accessing three coordinated amidate ligands, while being large enough to promote the formation of discrete monometallic species by discouraging bridging interactions.

The reaction of tetrakis(dimethylamido) titanium with three equivalents of *N*-(2,6-dimethylphenyl)benzamide yields an orange solid after removal of the volatiles (Scheme 2). Single crystals suitable for X-ray crystallography can be obtained from a layered toluene–pentane solution thereby confirming the monometallic tris(amidate) structure (Fig. 1).

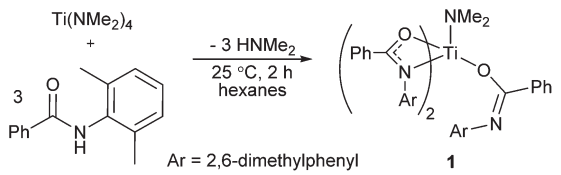

Scheme 2 Synthesis of tris(*N*-(2,6-dimethylphenyl)benzamidate) mono(dimethylamido) titanium **1**.

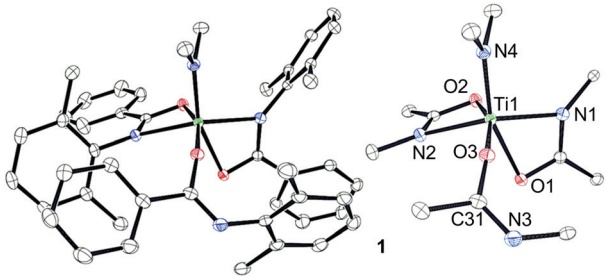

Fig. 1 ORTEP depiction of solid-state molecular structure of tris(amidate) complex **1**. Ellipsoids are plotted at 50% probability and hydrogen atoms are omitted for clarity, simplified core structure shown on the right. Selected bond lengths [Å] and angles [°]: Ti–N1 2.082(1), Ti–N2 2.149(2), Ti–N4 1.889(2), Ti–O1 2.137(1), Ti–O2 2.059(1), Ti–O3 1.857(1), C31–O3–Ti1 151.3(1), sum about N4 360°.

The amidate ligands in this species are non-equivalent, with two bound in a chelating κ^2 fashion while the third amidate ligand is monodentate. The κ^1-amidate ligand is bound *via* the more basic oxygen atom to this highly oxophilic hard metal centre. The formation of this six-coordinate titanium complex is not surprising, as expanded coordination numbers for titanium are less common, and the steric requirements of these amidate ligands are significant for this small metal centre.

Complex **1** exhibits distorted octahedral geometry with the amido ligand (N4) and the oxygen (O1) of one of the κ^2-bound amidates *trans* to one another. The steric properties of the amidate ligands affect the geometric isomer observed in the solid state, as to orient the bulky *N*-aryl substituents of the κ^2 ligands *trans* to one another. The Ti–O bond length of the κ^1-(*O*) amidate (1.857(1) Å) is considerably shorter than those of the κ^2 ligands (2.137(1) and 2.059(1) Å). While this short bond length could result from steric effects, the near linear angle (C31–O3–Ti1 151.3(1)°) of this κ^1-(*O*) bound ligand is consistent with a strongly π-donating alkoxide ligand. The Ti–N4 amido bond length (1.889(2) Å) is within the range expected for M–N multiple bonds.[26] The solid-state molecular structure of the related 16e$^-$ bis(*N*-(2,6-dimethylphenyl)benzamidate) bis(diethylamido) titanium complex has been reported previously.[26] Comparison of the bond lengths in the bis(amidate) structure to those of **1** indicate that addition of the third amidate ligand results in a shortening of the average κ^2 amidate Ti–N (2.116 *cf.* 2.293 Å) and lengthening of the Ti–O bonds (2.098 *cf.* 2.040 Å), presumably due to exchange of the 4e$^-$ donating amido ligand with the more strongly π-donating alkoxide ligand of the κ^1-(*O*) amidate as well as the increased steric congestion. The Ti–N4 amido bond length (1.889(2) Å) is very similar to those found in the bis(amidate) analogue (1.894(1) and 1.901(1) Å).[26]

The solution-phase ^{1}H NMR spectroscopy of **1** is also consistent with more than one ligand binding mode and displays very broad signals at room temperature highlighting the fluxional behaviour of the ligands on the NMR timescale. The broad signals can be attributed to rapid interconversion between the κ^1- and κ^2-binding modes in the solution phase. Variable temperature ^{1}H NMR spectroscopy (25–80 °C, see ESI†) resulted in coalescence and sharpening of the amidate signals, consistent with increased fluxionality and the appearance of averaged signals.

Zirconium, as a larger metal centre, is better suited for accommodating such steric congestion and is known to have expanded coordination numbers.[15,27,28] Indeed, the reaction of three equivalents of the amide proligand with one equivalent of tetrakis(dimethylamido) zirconium generated tris(amidate) zirconium complexes **2–4** (Scheme 3).

These complexes have a variety of steric and electronic properties in the distal backbone position (R^1, Scheme 3) as well as on the nitrogen-bound aryl substituent (R^2, Scheme 3). Complexes **2** and **3** have also been prepared from the corresponding bis(amidate) bis(dimethylamido) zirconium complexes *via* addition of another equivalent of the amide

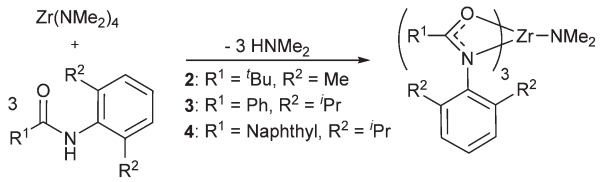

Scheme 3 Synthesis of tris(amidate) mono(dimethylamido) zirconium complexes **2–4**.

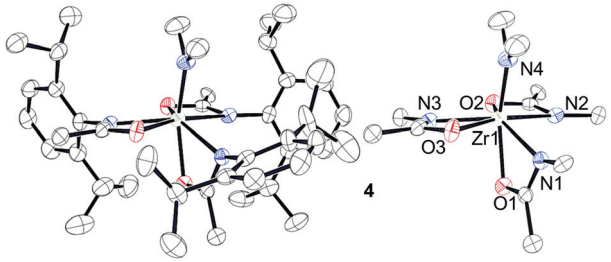

Fig. 2 ORTEP depiction of the solid-state molecular structure of tris(amidate) complex **4**. Ellipsoids plotted at 50% probability. The backbone naphthyl group and hydrogen atoms are omitted for clarity. Selected bond lengths [Å]: Zr–N1 2.431(3), Zr–N2 2.403(3), Zr–N3 2.271(3), Zr–N4 2.018(3), Zr–O1 2.151(2), Zr–O2 2.136(2), Zr–O3 2.208(2), sum about N4 360°.

proligand. A solid-state molecular structure was obtained for the sterically demanding complex **4** confirming that zirconium, as a larger metal centre, is capable of having all three amidates bound in a κ^2 manner (Fig. 2).

Complex **4** adopts a distorted pentagonal bipyramidal geometry in the solid state. The axial positions are occupied by the dimethylamido ligand (N4) and the oxygen (O1) of an amidate ligand. The remaining amidate donors (N1, N2, O2, N3, and O3) define the distorted pentagonal plane. The Zr–N4 amido bond (2.018(3) Å) is consistent with a Zr–N double bond.[26] Comparison to the related bis(*N*-(2,6-dimethylphenyl)-pivalamidate) bis(dimethylamido) zirconium[6] indicates that while the Zr–N dimethylamido bond length is shorter in the tris(amidate) **4** (2.018(3) *cf.* 2.038(3) and 2.044(2) Å), the amidate bond lengths on average are similar. Each of the amidate ligands in complex **4** are in different coordination environments. However, in every case the ligand is bound in an asymmetric fashion to the metal centre with a shorter Zr–O bond than Zr–N. The most symmetrically bound amidate (N3, O3) has a Zr–N and Zr–O bond length difference of 0.19 Å and the most asymmetric (N1, O1) has a difference of 0.28 Å. The bonding can therefore be most accurately described as an alkoxy–imine bonding mode, and **4** is considered to be a 16e$^-$ complex.

While the solid-state molecular structure of **4** demonstrates that this tris(amidate) complex is C_1-symmetric in the solid state, the room temperature ^{1}H NMR spectrum of **4** indicates a C_3-symmetric structure in solution, consistent with three equivalent κ^2-bound amidate ligands on the NMR timescale. The solution-phase spectroscopy of **2** is analogous, with one signal observed for the methyl substituents on the nitrogen-bound aryl substituent at δ 2.31 ppm. In contrast, **3**, with the more sterically demanding isopropylphenyl groups on the nitrogen-bound aryl substituent, exhibits hindered rotation leading to inequivalent isopropyl signals in the ^{1}H NMR spectrum.

The observed ligand fluxionality can result in disproportionation reactions in the solution phase. Indeed, while complexes **2–4** can be isolated readily, allowing the reaction (Scheme 3) to proceed for extended periods of time (>24 hours) can result in the formation of the bis(amidate) bis(amido) zirconium and tetrakis(amidate) complexes. This is particularly evident for complexes **3** and **4** which have the bulky diisopropylphenyl substituents on the nitrogen atom. This ligand redistribution is proposed to proceed *via* κ^1-bound amidate ligands that may engage in bridging interactions between metal centres. These examples of ligand redistribution point toward potential decomposition pathways for such systems. Notably, homoleptic amidate complexes can result in very sterically crowded 8-coordinate zirconium and hafnium complexes. To date, related homoleptic Ti species have not been observed.

The homoleptic complexes of both zirconium and hafnium can be synthesized with excellent yields of 85% and 94% respectively *via* protonolysis with the tetra(benzyl) metal precursors (Scheme 4). It is also possible *via* protonolysis with the tetrakis(dimethylamido) zirconium starting material, as has been shown for complex **5**. To date, no notable reactivity has been observed with these complexes; however, similar homoleptic small-bite-angle ligated early transition metals have been used as MOCVD precursors.[29–31] Solid-state structural data can be obtained for both Zr and Hf homoleptic compounds and show that **5** and **6** are isostructural, both adopting a dodecahedral geometry in the solid state with pseudo-D_{2d} symmetry (Fig. 3). For example, in complex **5** there exists the C_2-axis bisecting both N1 and N3, and N2 and N4. This axis also lies at the intersection of the two pseudo-mirror planes within the molecule. The two perpendicular C_2 axes of symmetry lie between the aforementioned mirror planes, bisecting O1 and O2, as well as O1 and O4. It must be noted that homoleptic hafnium complex **6** displays equivalent binding of all of the amidate ligands while those of complex **5** are slightly distorted. Each of the amidate ligands is once more bound in an asymmetric fashion to the metal centre with a shorter Zr–O bond compared with the Zr–N bond lengths (Δ 0.16–0.21 Å). The average metal to ligand bond lengths in the homoleptic structures (Zr–N 2.309, Zr–O 2.120 and Hf–N 2.325, Hf–O 2.163 Å) are slightly shorter than those in tris(amidate) **4** (Zr–N 2.368, Zr–O 2.164 Å).

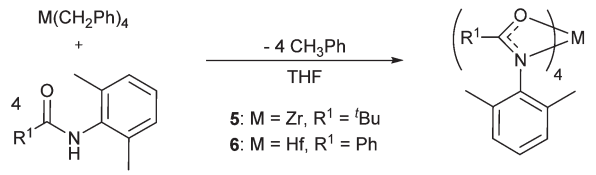

Scheme 4 Synthesis of homoleptic amidate complexes of zirconium and hafnium.

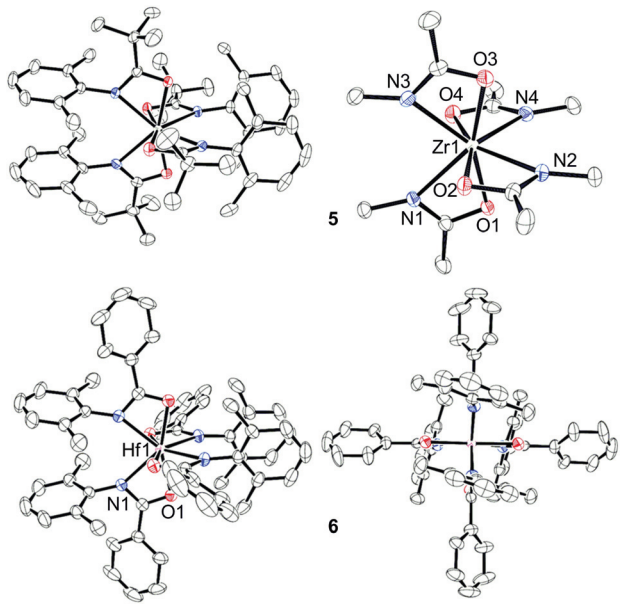

Fig. 3 ORTEP depiction of solid-state molecular structures of homoleptic amidate complexes **5** and **6**. Ellipsoids are plotted at 50% probability, and hydrogen atoms are omitted for clarity. Selected bond lengths for complex **5** [Å]: Zr–N1 2.323(1), Zr–N2 2.323(1), Zr–N3 2.295(2), Zr–N4 2.288(1), Zr–O1 2.120(1), Zr–O2 2.114(1), Zr–O3 2.124(1), Zr–O4 2.123(1). Selected bond lengths for complex **6** [Å]: Hf–N1 2.325(3), Hf–O1 2.163(3).

The most notable features of these complexes are the π-stacking interactions stabilizing the *N-cis* conformation, which would otherwise be sterically unfavourable (Table 1). The inter-ring distance from the ring centroids in complex **5** (3.610(3) Å) falls in the range typically expected for π-stacking (~3.6 Å)[32,33] while that of **6** (4.023(5) Å) is slightly longer. This is likely due to crystal packing resulting in the tilted nature of the aryl rings in complex **6**, demonstrated by the plane to plane angle of 15.4(3)°. It is also possible that the additional steric bulk of *tert*-butyl substituent on the backbone of **5** may force the two π-stacked rings closer together. High symmetry is observed in the solution-phase; the ^{1}H NMR spectra of **5** and **6** are consistent with all four ligands being equivalent. Variable temperature ^{1}H NMR spectroscopy of complex **6** did not show any discernible change over a wide range in temperatures.

With a thorough understanding of the solution-phase and the solid-state behaviour of these complexes, preliminary investigations into reactivity have been performed.

Table 1 π-Stacking interactions for tetrakis(amidate) complexes **5** and **6**[a]

	5 (Zr)	**6** (Hf)
Centroid–centroid (Å)	3.610(3) 3.615(3)	4.023(5)
Plane–plane angle (°)	3.96(15) 4.05(15)	15.4(3)
Plane–plane shift distance (Å)	1.207(7) 1.217(7)	1.583(9)

[a] Calculated using OLEX2.[34]

Reactivity and catalysis

These high-coordinate metal complexes have a large amount of steric bulk shielding the metal centre which could be detrimental for productive reactivity. Gratifyingly, reaction of the coordinatively saturated tris(amidate) complex **3** with aniline results in the formation of new tris(amidate) mono(anilido) complex **7** as a yellow microcrystalline solid (Scheme 5).

The ^{1}H NMR spectrum for complex **7** is very complicated, with hindered rotation about all three amidate N–C_{ipso} bonds which results in twelve distinct doublets and six septet resonances for the isopropyl methyl and methine protons respectively. Variable temperature ^{1}H NMR spectroscopy indicates a coalescence of the isopropyl methyl signals at high temperatures, and no significant change at low temperatures. Single crystals of **7** suitable for solid-state molecular structure determination can be isolated from a 1 : 1 toluene–hexanes mixture (Fig. 4).

The geometry of this compound is very similar to that of **4**, existing as a 7-coordinate complex best described as distorted pentagonal bipyramidal. In complex **7** however, the amidate axial position is occupied by the N2 donor, instead of an oxygen donor. The remaining amidate donors (N1, O1, N3, O3, and O2) define the pentagonal plane. Once again, the Zr–N4 amido bond (2.071(2) Å) is consistent with a Zr–N double bond and the κ^2-amidate ligands are bound to zirconium in an alkoxy–imine bonding mode.

This transamination reaction indicates that the amido group of these bulky systems is a reactive ligand and perhaps productive catalytic reactivity could be observed with these tris(amidate) zirconium complexes. One potential catalytic

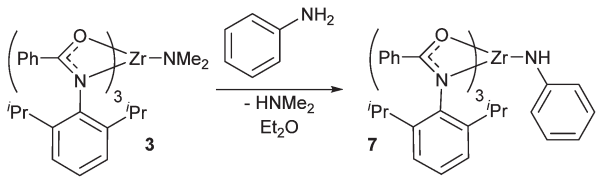

Scheme 5 Generation of **7** *via* reaction of **3** with aniline.

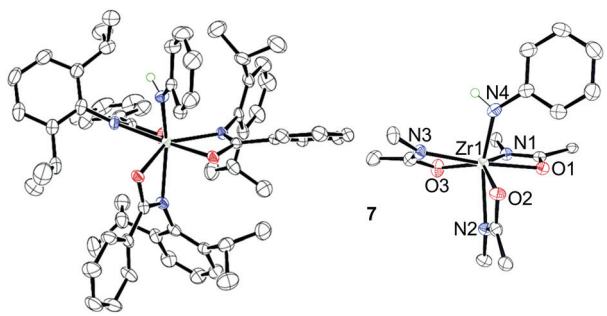

Fig. 4 ORTEP depiction of solid-state molecular structure of tris(amidate) complex **7**. Ellipsoids are plotted at 50% probability and hydrogen atoms are omitted for clarity. Selected bond lengths [Å]: Zr–N1 2.269(2), Zr–N2 2.340(2), Zr–N3 2.362(2), Zr–N4 2.071(2), Zr–O1 2.200(2), Zr–O2 2.144(2), Zr–O3 2.142(2), sum about N4 360°.

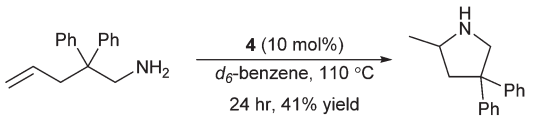

Scheme 6 Catalytic cyclohydroamination with precatalyst **4**.

application is hydroamination, as bis(amidate) supported group 4 systems for hydroamination have precedence in the literature.[4,6,8,21,24,35,36] To the best of our knowledge, tris(amidate) complexes of early transition metals have not been reported for this catalytic transformation.

For these studies we have focused on the use of precatalyst **4** (Scheme 4, Fig. 2), as the *ortho*-naphthyl ^{1}H NMR signal at δ 9.11 ppm of the *N*-(2,6-diisopropylphenyl)naphthylamidate ligand provides a convenient spectroscopic handle for monitoring ligand coordination. Interestingly, complex **4** is a successful, albeit sluggish, precatalyst for the cyclohydroamination of 2,2-diphenylpent-4-en-1-amine, a commonly used aminoalkene substrate[37] (Scheme 6). This C–N bond formation could be achieved with this very sterically shielded and coordinatively saturated metal centre in 41% NMR yield after 24 hours.[38]

This result was surprising considering that the majority of group 4 catalyzed hydroamination reactivity has been proposed to occur *via* a [2 + 2] cycloaddition between an imido–zirconium intermediate and the alkene.[39–45] Indeed early investigations are consistent with this cycloaddition-based mechanism for related bis(amidate) zirconium catalysts (Fig. 5).[21,22,39,44,45] However, the formation of the imido–zirconium intermediate requires the availability of two reactive ligand sites, which is not obvious with the three κ^2-bound amidate ligands in **4**.

Alternatively, there have been kinetic mechanistic as well as computational reports detailing zirconium precatalysts that promote this transformation *via* alternate mechanisms such as proton-assisted C–N bond formation or direct alkene insertion into the Zr–N bond of zirconium bis(amido) intermediates. These include zirconium complexes with constrained-geometry ligands,[46] zwitterionic complexes,[47] or a tethered bis(ureate) system.[15,48] However, such mechanistic pathways require a vacant coordination site in addition to the reactive Zr–N bond for coordinating either the incoming alkene (direct insertion) or the acidic amine (proton-assisted C–N bond formation). Precatalyst **4** does not afford a vacant coordination site in addition to the reactive Zr–N bond. However, such reactive species could be generated *in situ* by the ligand redistribution reactions detailed earlier or by substitution of an amidate ligand in the presence of excess amine.

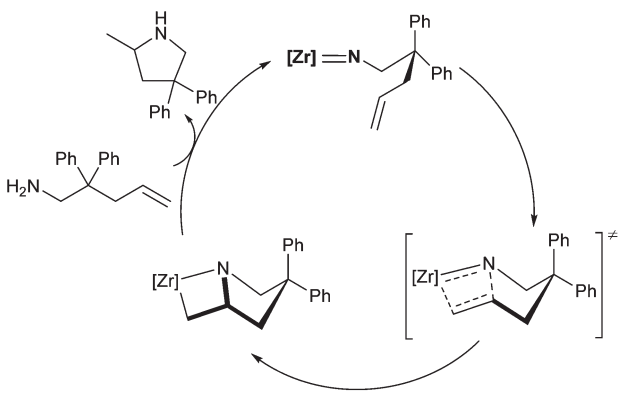

Fig. 5 Cycloaddition mechanism for zirconium catalyzed hydroamination supported by sterically bulky amidate ligands. [Zr] = bis(amidate) zirconium.

To probe the active species promoting the observed cyclohydroamination reaction, the reaction can be monitored by ^{1}H NMR spectroscopy as a function of time. After only 30 minutes at 110 °C there is the clear appearance of free ligand in the reaction mixture, as evidenced by the presence of a signal at δ 8.81 ppm, corresponding to the *ortho*-naphthyl signal of the *N*-(2,6-diisopropylphenyl)naphthylamide. Integration against the 1,3,5-trimethoxybenzene internal standard shows that one equivalent of free amide proligand is generated *in situ*. This protonolysis of an amidate ligand in the presence of excess amine would therefore generate bis(amidate) bis(amido) zirconium species in solution, which have been proposed to be active catalysts for hydroamination *via* the cycloaddition mechanistic pathway.[39] These observations are consistent with the observed induction period prior to productive reactivity (see ESI†) and can be attributed to the time required to generate active bis(amidate) complexes in solution.

Conclusions

The synthesis of tris(amidate) mono(amido) complexes of titanium and zirconium can be accomplished through protonolysis of tetrakis(amido) metal starting materials with amide proligands. These sterically demanding complexes have differing coordination modes depending on the size of the metal centre. When titanium is used, one of the amidate ligands is bound in a κ^1-(*O*) manner and the amidate ligands exhibit exchange between κ^1 and κ^2 modes on the ^{1}H NMR timescale. Zirconium and hafnium, as larger metal centres, can better accommodate the sterically demanding ligands, resulting in tris(amidate) and tetrakis(amidate) complexes with all amidate ligands bound in a κ^2 motif. The tris(amidate) complexes are susceptible to ligand exchange and disproportionation reactions and highlight the ligand fluxionality of amidate ligands in the solution phase. The propensity for ligand exchange to alleviate steric crowding can be used to access reactive complexes *in situ* for catalytic applications. The observed disproportionation into unreactive homoleptic species is noteworthy, and represents a potential catalyst decomposition pathway for amidate precatalyst systems.

Experimental procedures

General methods

All synthetic manipulations were conducted using conventional Schlenk line techniques or a glovebox under an atmosphere

of dry dinitrogen unless stated otherwise. Anhydrous hexanes and toluene were purchased from Aldrich, sparged with dry, degassed dinitrogen, and passed over an activated aluminum oxide column and degassed prior to use. Anhydrous benzene, diethyl ether, tetrahydrofuran, and pentanes were purchased from Aldrich, sparged with dry, degassed dinitrogen, and purified by passage through an Innovative Technologies SPS-PureSolv-400-4 apparatus. d_6-Benzene and d_8-toluene were purchased from Cambridge Isotopes Ltd, degassed by 3 freeze–pump–thaw cycles, and stored overnight over molecular sieves prior to use. Reagents for amide synthesis were used as received from Aldrich without further purification. The amides were synthesized from the corresponding commercial acid chlorides and amines and rigorously dried by heating to 100 °C under vacuum. The following compounds were synthesized as reported in the literature: *N*-(2,6-dimethylphenyl)-benzamide,[49] *N*-(2,6-dimethylphenyl)pivalamide,[23] *N*-(2,6-diisopropylphenyl)benzamide,[50] *N*-(2,6-diisopropylphenyl)naphthylamide,[23] 2,2-diphenylpent-4-en-1-amine,[51] $Zr(CH_2Ph)_4$,[52] and $Hf(CH_2Ph)_4$.[52] $Ti(NMe_2)_4$, $Zr(NMe_2)_4$, and $HfCl_4$ were purchased from Strem Chemicals and used as received. All NMR spectra were recorded on Bruker 300 MHz or 400 MHz Avance spectrometers in non-spinning mode and referenced to the residual solvent signal. Single crystal X-ray structure determinations, mass spectral, and elemental analyses determinations were performed at the Department of Chemistry, University of British Columbia. Mass spectra were measured on a Kratos MS-50. Elemental analyses were performed on a Carlo Erba Elemental Analyzer EA 1108. All X-ray crystallographic measurements were made on Rigaku ADSC, Rigaku AFC7, Bruker X8 APEX CCD, or Bruker APEX DUO area detectors with graphite-monochromated Mo K_α radiation. Crystals for X-ray diffraction studies were recrystallized from the indicated solvent, mounted in inert oil, and transferred to the cold gas stream of the diffractometer.

Synthesis of tris(*N*-(2,6-dimethylphenyl)benzamidate) mono(dimethylamido) titanium, 1. $Ti(NMe_2)_4$ (0.0668 g, 0.2981 mmol) was weighed out into a large vial equipped with a stir bar and ~3 mL of hexanes was added. A suspension of *N*-(2,6-dimethylphenyl)benzamide (0.2015 g, 0.8944 mmol) in hexanes was added slowly to the $Ti(NMe_2)_4$ solution and stirred for 2 h. The clear, orange/red solution was then concentrated to dryness *in vacuo* resulting in an orange powder. Recrystallization from a layered toluene–pentane solution gave **1** as red prisms (0.210 g, 92%). (Found: C, 74.00; H, 6.29; N, 7.32%. $C_{47}H_{48}N_4O_3Ti$ requires C, 73.81; H, 6.33; N, 7.33%); δ_H (400 MHz, C_6D_6, 85 °C), 2.26 (18H, s, Ar(CH_3)$_2$), 3.43 (6H, br s, N(CH_3)$_2$), 6.80–6.99 (18H, m, Ar-*H*), 7.65 (6H, br s, Ar-*H*); δ_C (125 MHz, C_6D_6, 85 °C)[53] 19.2, 51.0, 124.8 (br), 128.9, 129.2, 131.3 (br), 134.6 (br), 145.6 (br); MS(EI) *m*/*z* 764 ([M^+]), 721 ([M^+] − NMe_2), 540 ([M^+] − amidate), 496 ([M^+] − NMe_2 − amidate), 225 (amidate).

Crystal data. $C_{47}H_{48}N_4O_3Ti$, M = 764.79, monoclinic, a = 24.942(3), b = 10.581(1), c = 31.085(3) Å, V = 8203(2) Å^3, T = 90 K, space group $C2/c$, Z = 8, μ(Mo-Kα) = 0.25 mm^{-1}, 40 442 reflections measured, 10 639 unique (R_{int} = 0.042) which were used in all calculations. The final w$R(F^2)$ was 0.116 (all data).

Synthesis of tris(*N*-(2,6-dimethylphenyl)pivalamidate) mono-(dimethylamido) zirconium, 2. *N*-(2,6-Dimethylphenyl)pivalamide (2.30 g, 11.2 mmol) was dissolved in ~120 mL of toluene in a 250 mL round bottomed Schlenk flask and cooled to −78 °C while stirring. In a separate flask, $Zr(NMe_2)_4$ (1.00 g, 3.73 mmol) was dissolved in ~30 mL of Et_2O prior to addition to the solution of the amide *via* cannula. This solution was allowed to warm to room temperature overnight while stirring, resulting in a clear colourless solution. Excess solvent was removed *in vacuo* to generate an off-white waxy solid. The crude product was dissolved in 25 mL of pentane and filtered through Celite™ to remove traces of unreacted proligand. The solution was concentrated to dryness to give **2** (2.48 g, 89%). δ_H (300 MHz, C_6D_6) 1.02 (27H, s, C(CH_3)$_3$), 2.31 (18H, br s, Ph-(CH_3)$_2$), 2.96 (6H, s, N(CH_3)$_2$), 6.78 (9H, m, Ar-*H*). δ_C (75 MHz, C_6D_6): 19.6, 27.8, 41.3, 43.2, 124.3, 127.8, 132.4, 143.7, 189.6.

Synthesis of tris(*N*-(2,6-diisopropylphenyl)benzamidate) mono(dimethylamido) zirconium, 3. *N*-(2,6-Dimethylphenyl)-benzamide (3.15 g, 11.2 mmol) was dissolved in ~100 mL of Et_2O in a 250 mL round bottomed Schlenk flask and cooled to −78 °C while stirring. In a separate flask, $Zr(NMe_2)_4$ (1.00 g, 3.73 mmol) was dissolved in ~30 mL of Et_2O prior to addition to the solution of the amide *via* cannula. This solution was allowed to warm to room temperature overnight while stirring, resulting in a clear colorless solution. Excess Et_2O was removed *in vacuo* resulting in a white solid residue. The crude product was dissolved in 20 mL of pentane and filtered through Celite™ to remove traces of unreacted proligand. The solution was concentrated to dryness to give **3** (3.13 g, 86%). (Found: C, 71.47; H, 8.91; N, 5.20%. $C_{59}H_{72}N_4O_3Zr$ requires C, 72.57; H, 7.43; N, 5.74%.) δ_H (300 MHz, C_6D_6) 0.88 (18H, d, $^3J_{HH}$ = 6.4 Hz, CH(CH_3)$_2$), 1.07 (6H, d, $^3J_{HH}$ = 6.6 Hz, C(CH_3)$_2$), 1.26 (12H, d, $^3J_{HH}$ = 6.7 Hz, C(CH_3)$_2$), 3.29 (6H, s, N(CH_3)$_2$), 3.75 (6H, sept, $^3J_{HH}$ = 6.7 Hz, CH(CH_3)$_2$), 6.72–7.60 (24H, m, Ar-*H*). δ_C (75 MHz, C_6D_6): δ 24.9, 25.5, 28.7, 43.7, 124.8, 126.4, 128.3, 130.8, 131.9, 132.9, 142.6, 143.2, 178.1; MS(EI) *m*/*z* 930 ([M^+] − NMe_2).

Synthesis of tris(*N*-(2,6-dimethylphenyl)naphthylamidate) mono(dimethylamido) zirconium, 4. *N*-(2,6-Dimethylphenyl)-naphthylamide (0.40 g, 1.21 mmol) was dissolved in ~5 mL of THF in a 20 mL vial. In a separate Schlenk flask, $Zr(NMe_2)_4$ (0.109 g, 0.4 mmol) was dissolved in ~20 mL of THF prior to the addition of the ligand solution *via* pipette. The solution was warmed to 60 °C overnight and then filtered through a pipette plug of Celite™. The solution was concentrated to dryness, and washed with pentanes. The pentanes were then decanted off resulting in **4** as a white solid. (Found: C, 76.04; H, 7.36; N, 4.80%. $C_{71}H_{78}N_4O_3Zr$ requires C, 75.69; H, 6.98; N, 4.97%); δ_H (300 MHz, C_6D_6) 0.60 (18H, d, $^3J_{HH}$ = 6.1 Hz, CH(CH_3)$_2$), 1.16 (18H, d, $^3J_{HH}$ = 6.6 Hz, CH(CH_3)$_2$), 3.55 (6H, br s, N(CH_3)$_2$), 3.72–3.82 (6H, m, CH(CH_3)$_2$), 6.77 (3H, t, $^3J_{HH}$ = 7.5 Hz, Ar-*H*), 7.00 (9H, br s, Ar-*H*), 7.16–7.20 (3H, m, Ar-*H*), 7.33–7.47 (12H, m, Ar-*H*), 9.11 (3H, d, $^3J_{HH}$ = 8.6 Hz, Ar-*H*); δ_C (75 MHz, C_6D_6) 22.7, 24.0, 28.3, 44.2, 123.8, 124.2, 125.7,

126.0, 127.0, 127.3, 128.6, 130.2, 131.4, 132.0, 134.5, 141.2, 142.7, 180.8; MS(EI) *m/z* 1125 ([M$^+$]), 1081 ([M$^+$] − NMe_2), 750 ([M$^+$] − amidate − NMe_2).

Crystal data. $C_{71}H_{78}N_4O_3Zr$, M = 1126.59, triclinic, a = 11.9659(8), b = 12.5520(8), c = 23.178(2) Å, V = 3199.2(4) Å^3, T = 100 K, space group $P\bar{1}$, Z = 2, μ(Mo-Kα) = 0.22 mm^{-1}, 20 144 reflections measured, 8118 unique (R_{int} = 0.059) which were used in all calculations. The final w$R(F^2)$ was 0.094 (all data).

Synthesis of tetrakis((*N*-2,6-dimethylphenyl)pivalamidate) zirconium, 5. *N*-(2,6-Dimethylphenyl)pivalamide (0.77 g, 3.76 mmol) and $Zr(CH_2Ph)_4$ (0.25 g, 0.94 mmol) were combined in a foil wrapped 250 mL round-bottomed Schlenk flask equipped with a stir bar. To this flask was added 50 mL of THF which had been cooled to −78 °C. The cloudy white mixture was allowed to warm to room temperature and stirred overnight. The clear, colourless solution was concentrated to dryness *in vacuo* to give a white solid residue. The crude material was triturated with ∼30 mL of hexanes, and the product was isolated by filtration and dried *in vacuo* to give 6 as a white powder (0.72 g, 85%). Single clear colourless crystals suitable for X-ray crystallographic analysis were grown from a saturated hexane/benzene solution at room temperature. δ_H (300 MHz, C_6D_6) 1.02 (36H, s, C(CH_3)$_3$) 2.40 (24H, s, Ar(CH_3)$_2$), 6.62–6.69 (12H, m, Ar-*H*); δ_C (100 MHz, C_6D_6) 20.5, 28.3, 41.6, 124.7, 128.0, 132.8, 143.3, 189.9.

Crystal data. $C_{52}H_{72}N_4O_4Zr$, M = 908.36, triclinic, a = 11.901(2), b = 11.908(2), c = 18.614(3) Å, V = 2568.1(8) Å^3, T = 173 K, space group $P\bar{1}$, Z = 2, μ(Mo-Kα) = 0.26 mm^{-1}, 33 550 reflections measured, 12 691 unique (R_{int} = 0.031) which were used in all calculations. The final w$R(F^2)$ was 0.107 (all data).

Synthesis of tetrakis((*N*-2,6-dimethylphenyl)benzamidate) hafnium, 6. *N*-(2,6-Dimethylphenyl)benzamide (3.32 g, 14.7 mmol) and $Hf(CH_2Ph)_4$ (2.00 g, 3.68 mmol) were combined in a foil wrapped 500 mL round-bottomed Schlenk flask equipped with a stir bar. To this flask was added 100 mL of THF which had been cooled to −78 °C. The cloudy white mixture was allowed to warm to room temperature and stirred for 2 h. The clear, colourless solution was then concentrated to dryness *in vacuo* to give a white solid residue. The crude material was washed with ∼50 mL of hexanes and dried *in vacuo* to yield 7 as a white powder (3.72 g, 94%). Single clear colourless crystals suitable for X-ray crystallographic analysis were grown from a saturated hexanes solution at room temperature. (Found: C, 67.26; H, 5.37; N, 5.09%. $C_{60}H_{56}N_4O_4Hf$ requires C, 67.00; H, 5.25; N, 5.21%); δ_H (300 MHz, C_6D_6) 2.51 (24H, s, Ar(CH_3)$_2$), 6.77–6.87 (24H, m, Ar-*H*), 7.70 (8H, d, $^3J_{HH}$ = 6.5 Hz, Ar-*H*); δ_C (75 MHz, C_6D_6) 19.8, 125.3, 128.4, 128.8, 129.3, 132.0, 133.4, 134.5, 143.4, 179.2; MS(EI) *m/z* 1076 ([M$^+$]), 852 ([M$^+$] − [amidate]).

Crystal data. $C_{60}H_{56}HfN_4O_4$, M = 1075.56, tetragonal, a = 11.0080(7), b = 11.0080(7), c = 21.318(2) Å, V = 2583.2(5) Å^3, T = 173 K, space group $P\bar{4}2_1c$, Z = 2, μ(Mo-Kα) = 2.07 mm^{-1}, 20 445 reflections measured, 3104 unique (R_{int} = 0.072) which were used in all calculations. The final w$R(F^2)$ was 0.082 (all data).

Synthesis of tris(*N*-(2,6-diisopropylphenyl)benzamidate) mono(anilido) zirconium, 7. Complex **3** (1.00 g, 1.35 mmol) was dissolved in 100 mL Et_2O and cooled to −78 °C in a 250 mL round bottomed Schlenk flask. To this flask was added (0.1 mL, 1.35 mmol) aniline which had been dissolved in 10 mL of Et_2O. This solution was allowed to warm to room temperature overnight while stirring, resulting in a bright yellow solution. Excess Et_2O was removed *in vacuo* to generate a yellow solid residue. The crude product was dissolved in 15 mL of pentane and filtered through Celite™ to remove a small amount of pale yellow insoluble material. The solution was concentrated to dryness to give **5** as a bright yellow solid (0.700 g, 51%). Single crystals were grown from a saturated toluene solution at room temperature. δ_H (300 MHz, C_6D_6) −0.08 (3H, d, $^3J_{HH}$ = 6.7 Hz, CH(CH_3)$_2$), 0.18 (3H, d, $^3J_{HH}$ = 6.5 Hz, CH(CH_3)$_2$), 0.24 (3H, d, $^3J_{HH}$ = 6.6 Hz, CH(CH_3)$_2$), 0.48 (3H, d, $^3J_{HH}$ = 6.8 Hz, CH(CH_3)$_2$), 0.59 (3H, d, $^3J_{HH}$ = 6.5 Hz, CH(CH_3)$_2$), 0.82 (3H, d, $^3J_{HH}$ = 6.6 Hz, CH(CH_3)$_2$), 0.89 (3H, d, $^3J_{HH}$ = 6.5 Hz, CH(CH_3)$_2$), 1.08 (3H, d, $^3J_{HH}$ = 6.5 Hz, CH(CH_3)$_2$), 1.14 (3H, d, $^3J_{HH}$ = 6.7 Hz, CH(CH_3)$_2$), 1.30 (3H, d, $^3J_{HH}$ = 6.5 Hz, CH(CH_3)$_2$), 1.48 (3H, d, $^3J_{HH}$ = 6.7 Hz, CH(CH_3)$_2$), 1.81 (3H, d, $^3J_{HH}$ = 6.8 Hz, CH(CH_3)$_2$), 2.69 (1H, sept, $^3J_{HH}$ = 6.8 Hz, CH(CH$_3$)$_2$), 3.21 (1H, sept, $^3J_{HH}$ = 6.8 Hz, CH(CH$_3$)$_2$), 3.58 (1H, sept, $^3J_{HH}$ = 6.9 Hz, CH(CH$_3$)$_2$), 3.60 (1H, sept, $^3J_{HH}$ = 6.7 Hz, CH(CH$_3$)$_2$), 3.69 (1H, br s, CH(CH$_3$)$_2$), 4.54 (1H, sept, $^3J_{HH}$ = 7.6 Hz, CH(CH$_3$)$_2$), 6.57–7.71 (29H, m, Ar-*H*), 8.15 (1H, s, Zr-N*H*); MS(EI) (*m/z*): 930 ([M$^+$] − NHPh).

Crystal data. $C_{70}H_{80}N_4O_3Zr$, M = 1116.60, triclinic, a = 13.661(5), b = 15.314(5), c = 18.604(5) Å, V = 3395.0(19) Å^3, T = 173 K, space group $P\bar{1}$, Z = 2, μ(Mo-Kα) = 0.21 mm^{-1}, 41 052 reflections measured, 11 859 unique (R_{int} = 0.053) which were used in all calculations. The final w$R(F^2)$ was 0.115 (all data).

General procedure for the intramolecular hydroamination of primary aminoalkenes with complex 4

Complex **4** (10.0 mg, 0.0089 mmol), 2,2-diphenylpent-4-en-1-amine (21.1 mg, 0.089 mmol), 1,3,5-trimethoxybenzene (5 mg, 0.0296 mmol), and d_6-benzene (∼0.5 g) were weighed into a small vial and then transferred into a J. Young NMR tube equipped with a Teflon cap. The reaction mixture was heated in a pre-heated 110 °C oil bath for the indicated time and monitored by ^{1}H NMR spectroscopy.

Acknowledgements

The authors gratefully acknowledge Boehringer Ingelheim (Canada) Ltd and NSERC for supporting this work. PRP thanks NSERC for a graduate scholarship. The authors thank Scott Ryken, Jacky Yim, and Dr Brian O. Patrick for help with the X-ray crystallography studies.

References

1 P. Arndt, C. Lefeber, R. Kempe, A. Tillack and U. Rosenthal, *Chem. Ber.*, 1996, **129**, 1281–1285.

2 G. R. Giesbrecht, A. Shafir and J. Arnold, *Inorg. Chem.*, 2001, **40**, 6069–6072.
3 D. V. Gribkov and K. C. Hultzsch, *Angew. Chem., Int. Ed.*, 2004, **43**, 5542–5546.
4 P. D. Knight, I. Munslow, P. N. O'Shaughnessy and P. Scott, *Chem. Commun.*, 2004, 894–895.
5 D. A. Kissounko, I. A. Guzei, S. H. Gellman and S. S. Stahl, *Organometallics*, 2005, **24**, 5208–5210.
6 A. V. Lee and L. L. Schafer, *Eur. J. Inorg. Chem.*, 2007, 2243–2255.
7 A. L. Reznichenko and K. C. Hultzsch, *Organometallics*, 2010, **29**, 24–27.
8 P. Eisenberger and L. L. Schafer, *Pure Appl. Chem.*, 2010, **82**, 1503–1515.
9 F. Zhang, J. Zhang, H. Song and G. Zi, *Inorg. Chem. Commun.*, 2011, **14**, 72–74.
10 G. Zi, F. Zhang and H. Song, *Chem. Commun.*, 2010, **46**, 6296–6298.
11 P. Eisenberger, R. O. Ayinla, J. M. P. Lauzon and L. L. Schafer, *Angew. Chem., Int. Ed.*, 2009, **48**, 8361–8365.
12 L. J. E. Stanlake and L. L. Schafer, *Organometallics*, 2009, **28**, 3990–3998.
13 J. A. Thomson and L. L. Schafer, *Dalton Trans.*, 2012, **41**, 7897–7904.
14 R. L. Webster, N. Noroozi, S. G. Hatzikiriakos, J. A. Thomson and L. L. Schafer, *Chem. Commun.*, 2013, **49**, 57–59.
15 D. C. Leitch, P. R. Payne, C. R. Dunbar and L. L. Schafer, *J. Am. Chem. Soc.*, 2009, **131**, 18246–18247.
16 P. R. Payne, J. A. Bexrud, D. C. Leitch and L. L. Schafer, *Can. J. Chem.*, 2011, **89**, 1222–1229.
17 Z. Zhang and L. L. Schafer, *Org. Lett.*, 2003, **5**, 4733–4736.
18 C. Li, R. K. Thomson, B. Gillon, B. O. Patrick and L. L. Schafer, *Chem. Commun.*, 2003, 2462–2463.
19 A. L. Gott, A. J. Clarke, G. J. Clarkson and P. Scott, *Organometallics*, 2007, **26**, 1729–1737.
20 J. A. Bexrud and L. L. Schafer, *Dalton Trans.*, 2010, **39**, 361–363.
21 M. C. Wood, D. C. Leitch, C. S. Yeung, J. A. Kozak and L. L. Schafer, *Angew. Chem., Int. Ed.*, 2007, **46**, 354–358.
22 M. C. Wood, D. C. Leitch, C. S. Yeung, J. A. Kozak and L. L. Schafer, *Angew. Chem., Int. Ed.*, 2009, **48**, 6938.
23 L. J. E. Stanlake, J. D. Beard and L. L. Schafer, *Inorg. Chem.*, 2008, **47**, 8062–8068.
24 Z. Zhang, D. C. Leitch, M. Lu, B. O. Patrick and L. L. Schafer, *Chem.–Eur. J.*, 2007, **13**, 2012–2022.
25 H. Zhai, A. Borzenko, Y. Y. Lau, S. H. Ahn and L. L. Schafer, *Angew. Chem., Int. Ed.*, 2012, **51**, 12219–12223.
26 R. K. Thomson, F. E. Zahariev, Z. Zhang, B. O. Patrick, Y. A. Wang and L. L. Schafer, *Inorg. Chem.*, 2005, **44**, 8680–8689.
27 G. Willey, T. Woodman, M. Fisher and M. B. Drew, *Transition Met. Chem.*, 1998, **23**, 467–471.
28 R. Hart, W. Levason, B. Patel and G. Reid, *J. Chem. Soc., Dalton Trans.*, 2002, 3153–3159.
29 S. V. Pasko, A. Abrutis and L. G. Hubert-Pfalzgraf, *Mater. Lett.*, 2005, **59**, 261–265.
30 Y. F. Loo, R. O'Kane, A. C. Jones, H. C. Aspinall, R. J. Potter, P. R. Chalker, J. F. Bickley, S. Taylor and L. M. Smith, *J. Mater. Chem.*, 2005, **15**, 1896–1902.
31 G. I. Spijksma, H. J. M. Bouwmeester, D. H. A. Blank, A. Fischer, M. Henry and V. G. Kessler, *Inorg. Chem.*, 2006, **45**, 4938–4950.
32 H. W. Roesky and M. Andruh, *Coord. Chem. Rev.*, 2003, **236**, 91–119.
33 Q. F. Mokuolu, P. A. Duckmanton, P. B. Hitchcock, C. Wilson, A. J. Blake, L. Shukla and J. B. Love, *Dalton Trans.*, 2004, 1960–1970.
34 O. V. Dolomanov, L. J. Bourhis, R. J. Gildea, J. A. K. Howard and H. Puschmann, *J. Appl. Crystallogr.*, 2009, **42**, 339–341.
35 R. O. Ayinla and L. L. Schafer, *Inorg. Chim. Acta*, 2006, **359**, 3097–3102.
36 R. O. Ayinla, T. Gibson and L. L. Schafer, *J. Organomet. Chem.*, 2011, **696**, 50–60.
37 S. Hong and T. J. Marks, *Acc. Chem. Res.*, 2004, **37**, 673–686.
38 Determined using 1,3,5-trimethoxybenzene as an internal standard.
39 R. K. Thomson, J. A. Bexrud and L. L. Schafer, *Organometallics*, 2006, **25**, 4069–4071.
40 P. J. Walsh, A. M. Baranger and R. G. Bergman, *J. Am. Chem. Soc.*, 1992, **114**, 1708–1719.
41 F. Pohlki and S. Doye, *Angew. Chem., Int. Ed.*, 2001, **40**, 2305–2308.
42 J. S. Johnson and R. G. Bergman, *J. Am. Chem. Soc.*, 2001, **123**, 2923–2924.
43 Y. H. Li, Y. H. Shi and A. L. Odom, *J. Am. Chem. Soc.*, 2004, **126**, 1794–1803.
44 A. L. Gott, A. J. Clarke, G. J. Clarkson and P. Scott, *Chem. Commun.*, 2008, 1422–1424.
45 L. E. N. Allan, G. J. Clarkson, D. J. Fox, A. L. Gott and P. Scott, *J. Am. Chem. Soc.*, 2010, **132**, 15308–15320.
46 B. D. Stubbert and T. J. Marks, *J. Am. Chem. Soc.*, 2007, **129**, 6149–6167.
47 K. Manna, S. Xu and A. D. Sadow, *Angew. Chem., Int. Ed.*, 2011, **50**, 1865–1868.
48 D. C. Leitch, R. H. Platel and L. L. Schafer, *J. Am. Chem. Soc.*, 2011, **133**, 15453–15463.
49 R. K. Thomson, B. O. Patrick and L. L. Schafer, *Can. J. Chem.*, 2005, **83**, 1037–1042.
50 C. A. Nijhuis, E. Jellema, T. J. J. Sciarone, A. Meetsma, P. H. M. Budzelaar and B. Hessen, *Eur. J. Inorg. Chem.*, 2005, 2089–2099.
51 S. W. Hong, S. Tian, M. V. Metz and T. J. Marks, *J. Am. Chem. Soc.*, 2003, **125**, 14768–14783.
52 U. Zucchini, E. Albizzati and U. Giannini, *J. Organomet. Chem.*, 1971, **26**, 357–372.
53 Carbonyl carbon signal was not observed.